



## Numerical investigation on the effects of fueling the Turbulent Jet Ignition gas engine with methane and hydrogen

Ireneusz Pielecha<sup>a,\*</sup> , Filip Szwajca<sup>a</sup> , Kinga Skobiej<sup>a</sup> 

<sup>a</sup> Faculty of Civil and Transport Engineering, Poznan University of Technology, Poland

### ARTICLE INFO

Received: 31 October 2023  
Revised: 27 November 2023  
Accepted: 30 November 2023  
Available online: 30 November 2023

### KEYWORDS

Hydrogen engine  
Engine simulation  
Hydrogen and methane combustion  
Combustion indicators  
Turbulent Jet ignition engine

*The modern solution of two-stage combustion, namely the Turbulent Jet Ignition (TJI), enables the combustion of ultra-lean mixtures. Thanks to this solution, it became possible to reduce fuel consumption and, at the same time, to increase the combustion process indicators (including the overall combustion system efficiency). The article presents the results of numerical tests of a heavy-duty engine equipped with the TJI system running on gas fuels. The AVL BOOST software was used to analyze the effects of different fuel injection rates into the pre-chamber and various ignition timing angles, while maintaining a constant global excess air ratio. Increasing the proportion of hydrogen in the pre-chamber resulted in its reduction in the main chamber (the fuel dose was kept constant with different excess air coefficients in each of the chambers). The maximum combustion pressure values in both chambers were investigated. Changes in the amount of heat released and its release rate were determined. As a result of the simulations, different ignition and combustion conditions were presented for the tested fuels. Based on this, maps of fuel dose to prechamber vs. ignition advance angle were drawn up, showing selected thermodynamic indicators of the combustion process.*

This is an open access article under the CC BY license (<http://creativecommons.org/licenses/by/4.0/>)

## 1. Introduction

Reducing emissions of exhaust components is forcing the development of internal combustion engines and vehicle propulsion systems. For this reason, hybrid and electric drives are being developed, which can be a substitute for vehicles powered by typical internal combustion engines. Conventional motoring still uses fossil fuels, which include the main gasoline and diesel, and alternative fuels such as methane and ethanol. Increasingly, hydrogen is now being used, which can be extracted in various ways (resulting in a "colorful" division of hydrogen extraction) [11]. Hydrogen as a fuel is currently used in both internal combustion engines and fuel cells. Hydrogen can be burned in the internal combustion engines of heavy-duty vehicles (including rail vehicle engines) as a:

- co-combust with diesel fuel (in multi-fuel systems),
- the combustion of hydrogen in engines on so-called mono-fuel supply.

The Organization of the Petroleum Exporting Countries (OPEC) claims that the global diesel and gas-oil demand will increase from 28.6 to 31.6 million barrels/day between 2017 and 2040 [23].

With the growing demand for these middle distillates, the number of diesel-fueled light- and heavy-duty vehicles in the manufacturing, agricultural, and service sectors is expected to rise substantially [5]. Accurize Market Research Reports & Consulting Services [1] notice that the global market for diesel-powered engines will grow from 8.1 USD billion in 2018 to 11.02 USD billion in 2026.

Dual-fuel diesel engines also co-combust gaseous fuels [8]:

- LPG (liquefied petroleum gas)
- methane
- hydrogen
- or other fuels.

Most commonly, diesel is the pilot dose, as it does not require the installation of an ignition system.

\* Corresponding author: [ireneusz.pielecha@put.poznan.pl](mailto:ireneusz.pielecha@put.poznan.pl) (I. Pielecha)

Adding hydrogen gas to a diesel (DF) engine's combustion can enhance the combustion process and increase engine performance [12, 27, 33]. On the other hand hydrogen gas is one of the future fuels for the automotive industry because it is a clean and renewable fuel that can be extracted from the environment [35]. Based on its properties, hydrogen fuel has an autoignition temperature of 585°C, which enables its use in high compression engines like diesel engines [20].

Simulation studies of a dual-fuel diesel-hydrogen system were conducted by Ramsay and Dinesh [19] using direct injection of DF and late injection of hydrogen. The pilot dose contained only up to 5% energy. Four phases of combustion were distinguished: a) gaseous jet ignition delay, b) free-jet combustion, c) wall-jet combustion, and d) late combustion phases. Ignition is rapid with little to no premixed combustion present with hydrogen showing shorter ignition delay times than methane. Free-jet combustion is the phase before the jet contacts the chamber walls with the end of the phase being signalled by the quenching of the front of the non-premixed flame at the chamber walls leading to a reduction in its volume and thus fall off from peak heat release rate (HRR). Wall-jet combustion begins with the jets first impingement on the chamber wall. The late combustion phase begins after the injection event has ended and HRR begins to fall off rapidly.

Research on biodiesel-hydrogen mixtures was conducted by Winangun et al. [29]. The research was conducted on palm oil biodiesel and hydrogen using dual-fuel diesel engines. The results indicated that the addition of hydrogen gas could enhance the combustion characteristics of biodiesel, resulting in a shorter ignition delay and a 10% decrease in knock value compared to biodiesel.

In work conducted by Cernat et al. [3], it was found that the the values of maximum pressure rise rate start to increase for hydrogen addition, in correlation with the increase of fuel amount burned into the premixed stage, without exceed the normal values

domain with assure the normal and reliable engine operation.

Increasing attention is being paid to dual-fuel engines fueled by ammonia and hydrogen. An extensive review of such technology is given in the work [18]. The authors [14] presented the use of a dual-fuel engine fueled by these fuels with reactivity-controlled turbulent jet ignition (RCTJI). The low exhaust temperature of ammonia-hydrogen combustion also presents a challenge for the high-efficiency operation of aftertreatment systems. The use of oxygenated catalytic thermal reforming and electric assisted heating during hydrogen on-board production can increase exhaust gas temperatures, aiding the efficient operation of aftertreatment catalysts.

Single-fuel combustion of hydrogen in the engine significantly reduces emissions of carbon-containing components (CO, CO<sub>2</sub> and HC). Nitrogen oxides are becoming a significant problem. Hydrogen can be fed to the engine in both indirect and direct injection systems. With the latter method significantly increasing operating rates: up to 17%, with complete elimination of flame retraction [28, 34].

A two-stage combustion system with pre-chambers can be used to burn hydrogen (Fig. 1). These systems can be active (fuel supplied to and ignited in the chamber) and passive (ignition in the prechamber, fuel is not separately supplied to prechamber). Passive systems are characterized by a much smaller range of charge depletion. An extensive analysis of these systems was presented by Alvarez et al. [2]. It was found that this system (TJI) allows the combustion of lean mixture (variable gas) with an excess air ratio of 2.2 (conventional combustion system – 1.4).

Pre-production solutions for internal combustion engines were presented by companies (Fig. 2): Toyota [26], Yamaha [24], Mahle [17] and AVL [25] in automotive vehicles. HD vehicle engines were presented by: Keyou [21], Cummins [4], GM, Hyundai, Kubota, FEV [16] and Rolls-Royce (turbojet engine). Some of these engines can be successfully used in rail traction.

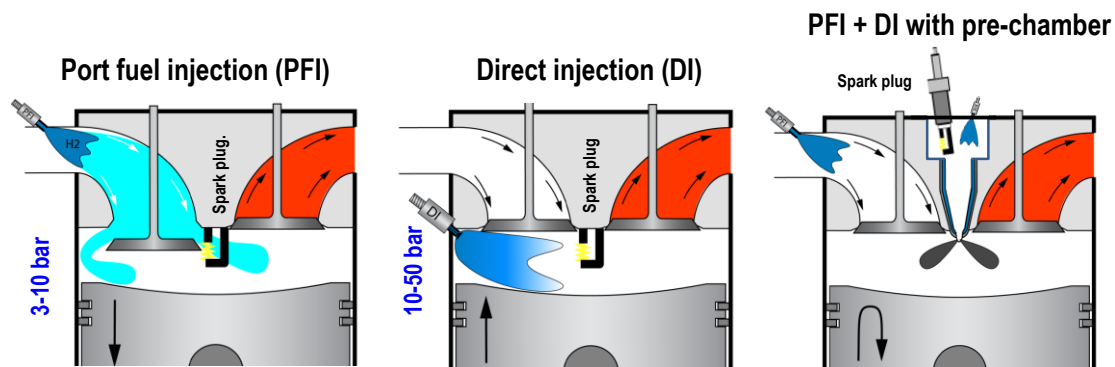


Fig. 1. Combustion systems of modern engines (based on [10])

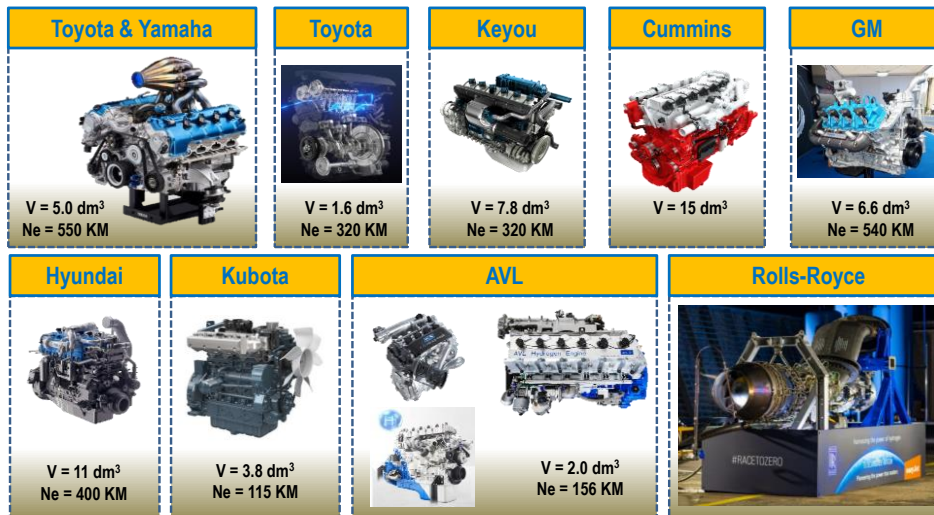


Fig. 2. Contemporary proposals for hydrogen-powered engines

## 2. Objective of the study

The purpose of the research work is to determine the differences in the combustion process of methane and hydrogen. The properties of these fuels allow a preliminary assessment of the combustion process, but prechamber combustion requires full research and simulation analysis. The completely different stoichiometric air requirements for fuel combustion make simulation studies very legitimate to obtain detailed information about the combustion process.

## 3. Methodology of work

### 3.1. Combustion chamber model

Simulation studies were conducted using a combustion chamber model equipped with an active prechamber of the Turbulent Jet Ignition system. The research work was conducted using AVL BOOST software (R2022.1). The software used a model of a single-cylinder internal combustion engine (Fig. 3a) with the intake and exhaust systems. The main component of the model is a cylinder with an active chamber attachment function. This allowed the use of the Pre-Chamber Spark Ignited Gas Engine (PCSI) combustion model. The same computational model was used for both fuels.

A prechamber (Fig. 3b) with a defined shape was implemented in an internal combustion engine with dimensions shown in Table 1. The operating conditions of the heavy-duty engine (HD) at  $n = 1500$  rpm with a prechamber with 8 holes were analyzed.

The model required adopting the geometry of the basic engine systems. Technical data of the engine, including the prechamber were implemented (Table 1). At the same time, the initial conditions of the simulation model were adopted (Table 2).

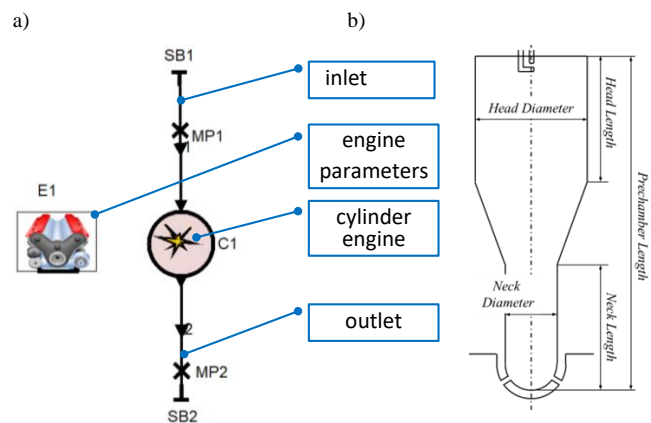


Fig. 3. Simulation model of the engine: a) diagram of the model, b) shape of the prechamber

Table 1. Technical data of the engine model

Parameter	Value
Engine	
Engine speed	1500 rpm
Bore × stroke	180 × 230 mm
Compression ratio	10
Conrod length	360 mm
Ignition angle	variable; dependent on fuel type
Piston bowl diameter	0.1 m
Piston bowl depth	0.02 m
TDC piston to head distance	0.0025 m
Prechamber	
Prechamber length	0.02 m
Neck diameter	15 mm
Number of holes	8 (the angle between the holes is 120 degrees – Fig. 3b)
Hole diameter	1.5 mm
Combustion model	PCSI
Fuel mass/cycle	variable; dependent on fuel type
Global $\lambda$	~ 1.7

Table 2. Initial simulation conditions for the single-cylinder model

Pressure	3 bar
Temperature	821 deg C
Fuel mass in main chamber	variable; dependent on fuel type (results from the demand for constant energy of fuel supplied)
Fuel temperature	25 deg C

The engine model adopted is a one-dimensional system. The simulations carried out involve one-dimensional modeling, which means that there is no spatial modeling of thermodynamic processes. This approach, on the one hand, simplifies modeling, while on the other hand, it leads to results that, at a further stage of design and simulation work, contribute to the detailing of 3D modeling (spatial modeling). AVL FIRE software can be used for this stage of modeling and simulation. An example of a 3D visualization of a combustion system with a prechamber implemented is shown in Fig. 4. This approach allows a preliminary analysis of the adopted design. The valves and pre-chamber system can be used for both automotive and HD vehicle engines. This means that they can be used for rail vehicle engines. The TJI system is not limited to a particular group of vehicles, and implementation in high-powered engines is easier. This is due to the availability of space for the use of a prechamber in the engine head. In addition, it is possible to fully liquid-cool it, which allows significant thermal load relief on the ignition system.

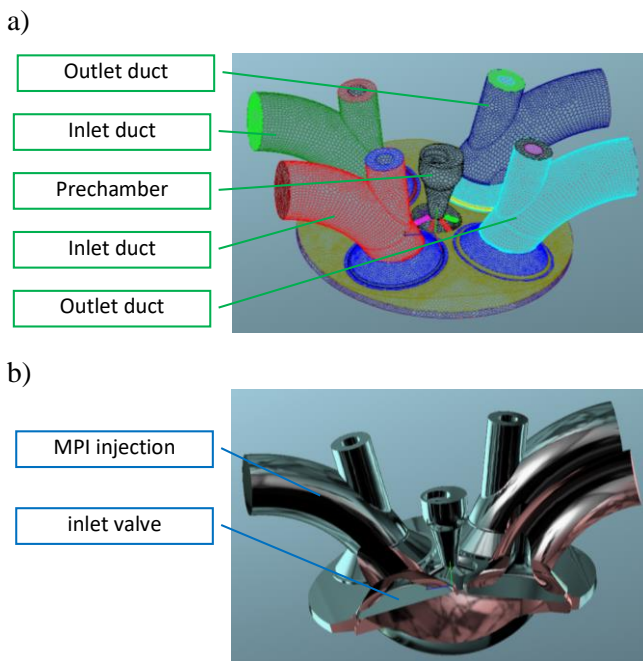


Fig. 4. An example of combustion chamber: a) chamber with intake and exhaust system and prechamber; b) view of valves and prechamber and main chamber (hemi)

Injection rate into the prechamber was determined according to a simplified triangular fuel injection model (Fig. 5). Fuel was injected into the prechamber with a certain angular advance of 90 deg bTDC. The injection time was 10 deg.

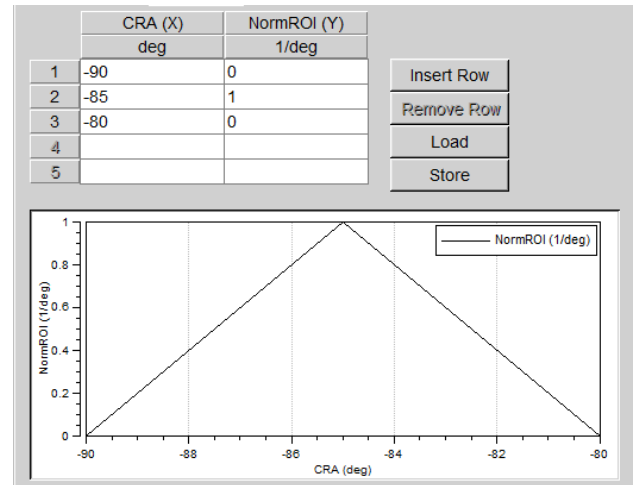


Fig. 5. Fuel injection model (hydrogen or methane)

### 3.2. Scope of work

It was assumed the tests would be conducted at a constant value center of combustion (CoC) around 5°CA aTDC. The angle for which 50% of the fuel dose was burned off was assumed as the center of combustion or CA50. For this reason, the IMEP (indicated mean effective pressure) value is the resulting parameter.

The research was carried out according to the following scheme, in which the variables were:

- fuel dose injected to the prechamber (1, 3, 5, 7%), which simultaneously forced changes in the main dose for both fuels
- ignition angle in a small range of changes: for hydrogen (5, 6, 7°CA before TDC) and for methane (15, 16, 17°CA bTDC) to achieve a CoC around 5°CA aTDC.

Research on the combustion process with an active pre-combustion chamber was conducted using methane and hydrogen. Combustion of methane in a two-stage TJI system is widely used in stationary engines. In this way, it is possible to use lean mixtures up to  $\lambda = 2$ . Another solution under study is the much less common combustion of pure hydrogen. Its use makes it possible to increase the depletion of the charge to  $\lambda = 4$ . Such a process makes it possible that the only harmful combustion products are nitrogen oxides (not including hydrocarbons and carbon monoxide formed in the combustion process from engine oil). The basic parameters of the fuels used are shown in Table 3.

Table 3. Characteristics of the fuels used in the simulation studies [7, 15, 22, 32]

Property	Methane	Hydrogen
Density [kg/m <sup>3</sup> ]	0.68	0.09
Laminar burning velocity [m/s]	0.4	3.1
Minimum spark ignition energy [mJ]	0.210	0.016
Flammable range [% vol]	4.4–17.0	4.0–75.0
Autoignition temperature [K]	813	858
Flame temperature in air [K]	2148	2318
Burning velocity in normal temperature and pressure air [cm/s]	45	325
Methane number	100	0
Higher heating value [MJ/m <sup>3</sup> ]	39.8	12.7
Lower heating value [MJ/m <sup>3</sup> ]	35.8	10.8

### 3.3. Equations and formulas

The discrepancies obtained during the cylinder pressure analysis were also confirmed during the heat release rate (HRR) test. This value was determined based on [9, 31]:

$$HRR = \frac{\kappa}{\kappa-1} \left( \frac{P_n + P_{n+1}}{2} \right) (V_{n+1} - V_n) + \frac{1}{\kappa-1} \left( \frac{V_n + V_{n+1}}{2} \right) (P_{n+1} - P_n) \quad (1)$$

where the average value of the polytropic index was assumed as  $\kappa = 1.32$  and the indices  $n$  and  $n + 1$  denote the current and the next pressure value in the cylinder ( $P$ ) or the corresponding cylinder volume ( $V$ ) and the HR (heat released) is given by [20]:

$$HR = \int_{SOC}^{EOC} \frac{HRR}{d\alpha} d\alpha \quad (2)$$

where: SOC – start of combustion, EOC – end of combustion.

Modeling of heat release is based primarily on the Wiebe function [13]:

$$f = 1 - \exp \left[ -a \left( \frac{\varphi - \varphi_0}{\Delta\varphi} \right)^{m+1} \right] \quad (3)$$

where  $f$  – is the share of the fuel dose that has been burned,  $\varphi$  – crankshaft angle,  $\varphi_0$  – crankshaft angle value at the start of ignition,  $\Delta\varphi$  – combustion duration,  $a$  – coefficient describing the degree of fuel use ( $a = 6.906$ ),  $m$  – coefficient characterizing the dynamics of the combustion process.

The modeling of heat release rates in the prechamber and main chamber follow a similar pattern, but their intensity and angle of occurrence are different (Fig. 6). The rate of heat release in the prechamber occurs much earlier (Fig. 6a), while at the same time the amount of heat released occurs at different crank angles (Fig. 6b).

The value of mass fraction burned (MFB) can be calculated as [6]:

Angle of burnout 5% of the total fuel dose:

$$MFB05(\alpha) = 0.05 \times \int_{SOC}^{EOC} \frac{dQ_{net}}{d\alpha} d\alpha \quad (4)$$

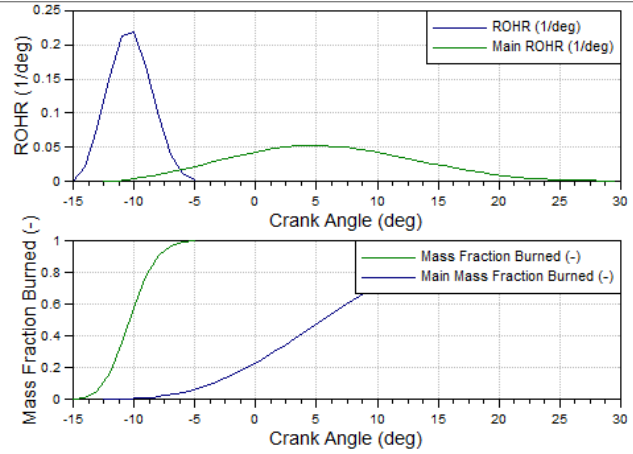


Fig. 6. Relative values of the rate of heat release (a) and the accumulated heat (b) during model tests of the combustion process

Center of combustion:

$$MFB50(\alpha) = 0.5 \times \int_{SOC}^{EOC} \frac{dQ_{net}}{d\alpha} d\alpha \quad (5)$$

Angle of burnout 95% of the total fuel dose:

$$MFB95(\alpha) = 0.95 \times \int_{SOC}^{EOC} \frac{dQ_{net}}{d\alpha} d\alpha \quad (6)$$

## 4. Analysis of thermodynamic indicators

### 4.1. Cylinder pressure

Analysis of the hydrogen and methane combustion pressures indicates different ignition conditions (Fig. 7 and 8). This is particularly marked with regard to the processes occurring in the prechamber. For a constant value of CoC for both fuels, hydrogen ignition occurs much later than during methane combustion. The difference is about 10°CA in order to achieve a similar maximum pressure location (Fig. 7a and 8a). With similar excess air ratios ( $\lambda \sim 1.7$ ), the maximum hydrogen combustion pressure is higher. The combustion of methane under lean conditions in a system with an undivided combustion chamber (without a prechamber) due to insufficient ignition energy is unfavorable. The excess air is too large for the homogeneous lean mixture to burn properly. When using a pre-chamber, in which ignition occurs under conditions similar to stoichiometric combustion, such irregularities do not occur. The combustion of hydrogen relative to methane is characterized by much wider flammability limits in the excess air ratio range up to  $\lambda = 4$ . Small changes in the ignition angle of hydrogen result in about 5% changes in maximum pressure. The same changes in the ignition timing of methane result in very similar maximum pressure differences of 5% as well.

The effect of fuel dose to the prechamber is more significant in the case of methane fueling (Fig. 7b and 8b). The analyzed model shows much less sensitivity

relative to hydrogen. When burning methane, the change in Pmx is about 5%, while practically no change is observed when burning hydrogen. This is due to the fact that a change in the methane dose to

the prechamber causes a much larger change in the excess air ratio in this area than when burning hydrogen. This effect is derived from the wider flammability limits of hydrogen mixtures relative to methane.

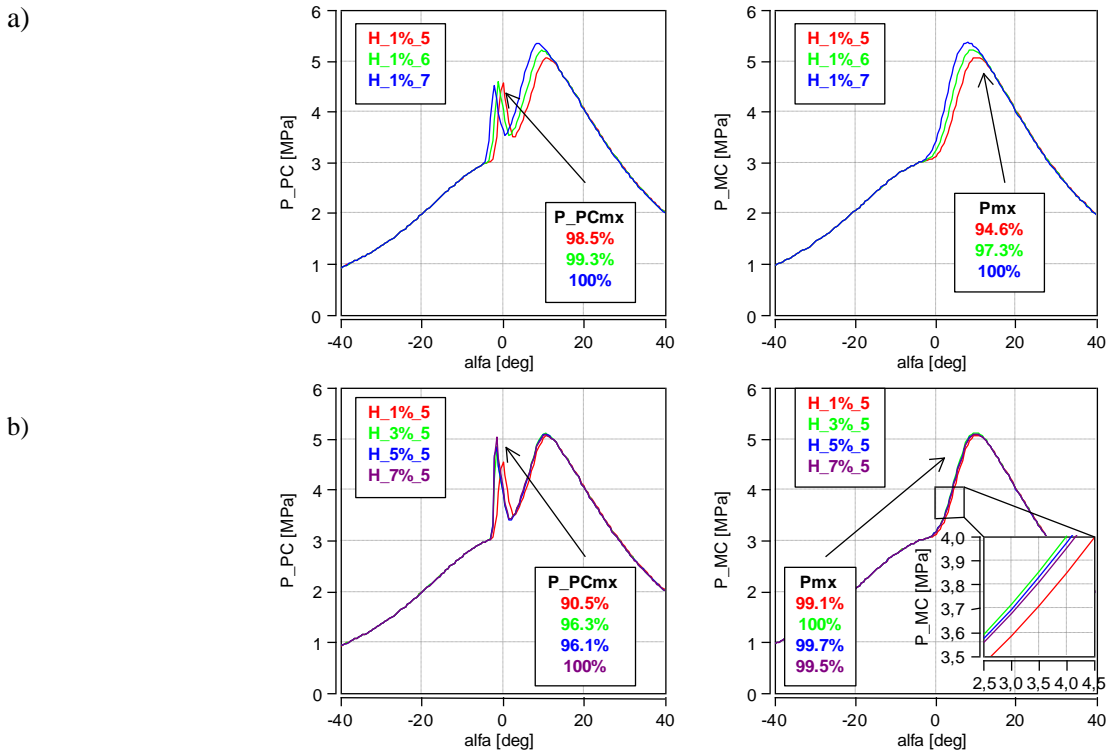


Fig. 7. Effect of ignition advance angle on cylinder pressure (MC) and prechamber pressure (PC) during hydrogen combustion: a) evaluation of the effect of changing the ignition angle, b) evaluation of the change in fuel dosage

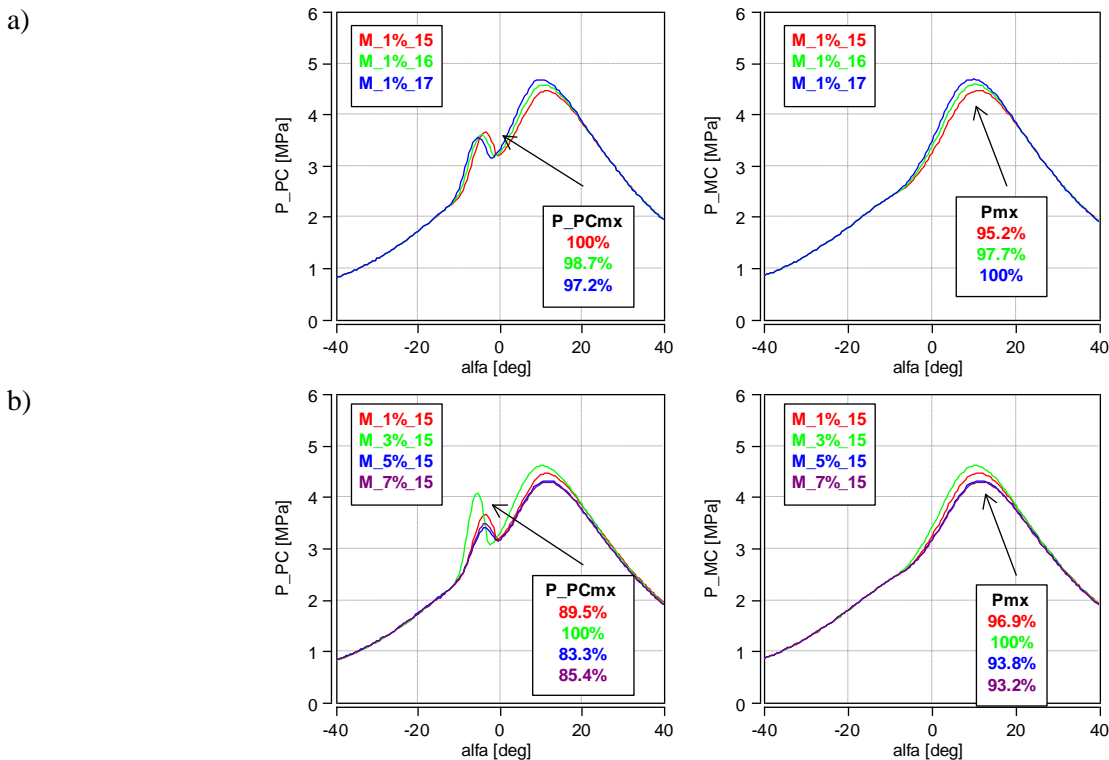


Fig. 8. Effect of ignition advance angle on cylinder pressure (MC) and prechamber pressure (PC) during methane combustion: a) evaluation of the effect of changing the ignition angle, b) evaluation of the change in fuel dosage

The combustion of methane as a gas is also slower than the combustion of hydrogen. For this reason, the pressure change in the prechamber is also less intense. The pressure maximum in the PC (prechamber) is much lower than during hydrogen combustion.

#### 4.2. Analysis of heat release

The rate of heat release was determined based on equation (1), and the cumulative heat released was determined based on equation (2) also taking into account the Wiebe – eq. model (3).

Analysis of the cumulative heat released (Fig. 9) indicates similar amounts of heat, which was realized by changing the value of the fuel dose. The prechamber was handled in a similar way: it was fed with 1% of the dose – the same values of the amount of heat released – 100 J (variable HR\_PC in Fig. 9) – are

derived from this. Similar fuel injection conditions in the prechamber resulted in similar heat release conditions in the prechamber. However, these conditions are different in the main chamber. Much faster combustion is seen when burning hydrogen. This results in an ignition angle that required a significant delay compared to the combustion of methane.

A detailed analysis of the cumulative heat released (Fig. 10) when changing the fuel dose to the prechamber shows that during hydrogen combustion, the ignition timing is more affected by changes than the amount of dose. The combustion of methane is slower as evidenced by the lower slope of the heat release curves. At the same time, changing the ignition timing or the dose in the prechamber significantly affects the course of heat release.

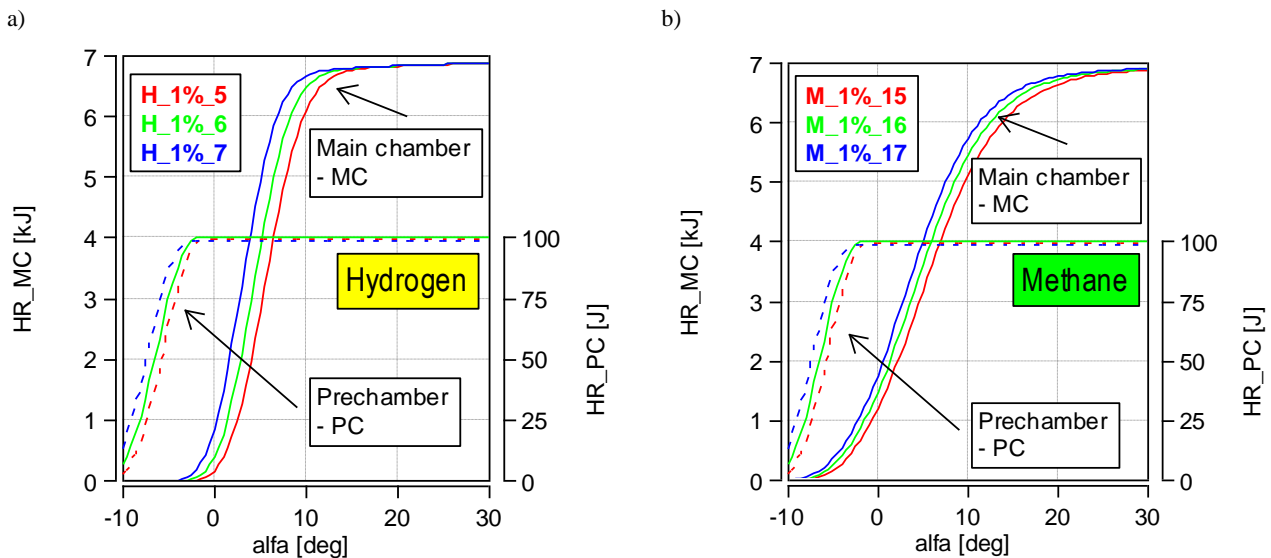


Fig. 9. Influence of ignition advance angle on in-cylinder heat release (MC) and prechamber (PC) values during combustion of: a) hydrogen, b) methane

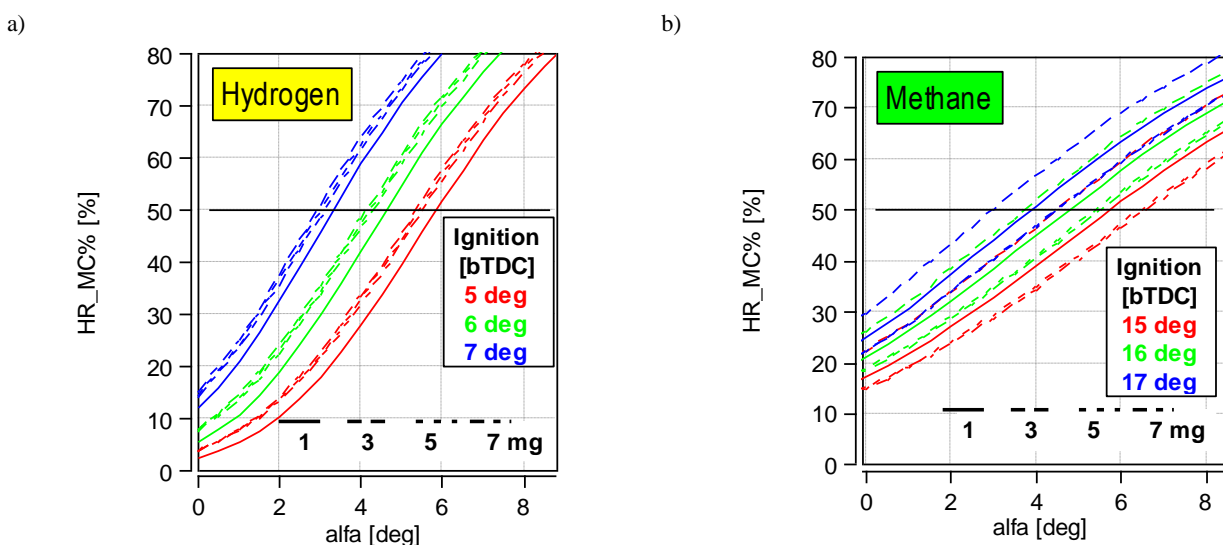


Fig. 10. CA50 analysis during combustion of: a) hydrogen, b) methane

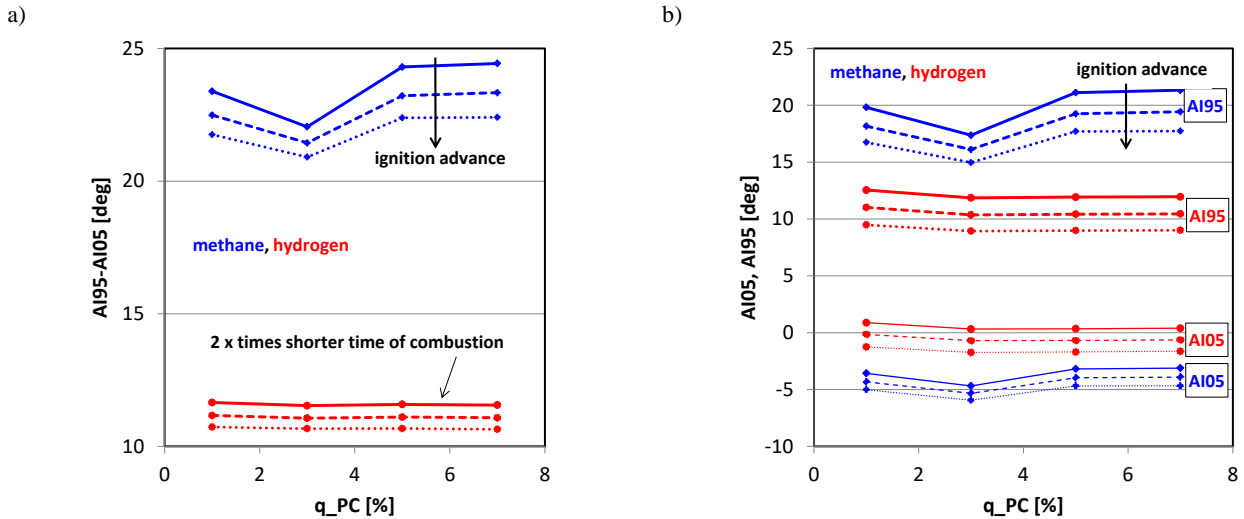


Fig. 11. Analysis of hydrogen and methane combustion: a) changes in the beginning and end of combustion, b) changes in the combustion time of both fuels

Such changes mean that the hydrogen combustion process can be controlled mainly by changing the ignition timing, while during methane combustion it is possible to control both the dose rate as well as the ignition timing. It should be noted that regardless of the conducted changes in dose settings or ignition timing, the values of the center of combustion – CoC (determined from equation (5)) are in the range of 3–6 deg aTDC.

An analysis of the combustion indicators determined from equations (4)–(6) is shown in Fig. 11. The analysis was carried out taking into account the previous settings, that is, maintaining a constant value of the CoC (about 6°CA aTDC). Such conditions required significant ignition advance during methane combustion. Nevertheless, the onset of combustion is ahead of that of hydrogen by about 5 deg. These values do not change significantly with respect to increasing fuel dose in the prechamber (Fig. 11a). With hydrogen fueling, the start of combustion is later, and the end of combustion is earlier. The end of methane combustion is delayed by about 7–8°CA with respect to the end of hydrogen combustion. Analysis of the combustion time of both fuels shows that hydrogen burns much faster (Fig. 11b): the difference is about 10 deg.

## 5. Thermodynamic indicators – contour maps

Engine operating maps refer to the thermodynamic indicators of the an internal combustion engine cycle, which are the combustion pressures in both the prechamber and main chamber. These maps were created in the fuel dose to PC-ignition timing (Fig. 12). Analysis of the maximum cylinder pressure during hydrogen indicates higher  $P_{mx}$  values in the main chamber than in the prechamber. The maximum pressure in the

main chamber increases with the advance of the ignition timing (Fig. 12a). The highest values are reached at about 3% dose to PC. The pressure in the prechamber reaches its highest value at the smallest ignition advance value ( $\alpha_{ign} = 5^\circ\text{CA bTDC}$ ) and also at a prechamber fuel dose of about 3% (Fig. 12b).

During methane combustion, the highest pressure in the main chamber is reached at the largest ignition advance timing and a dose equal to 3% (Fig. 12c). The pressure distribution field has a similar shape in the prechamber (Fig. 12d). The distribution of combustion pressure when burning methane and hydrogen in the prechamber is very similar.

A map of the temperature distribution in the two chambers during the combustion of both fuels is included in Fig. 13. The temperature maps show a high correspondence with the pressure distribution – correlations are converging. The temperature in the prechamber during hydrogen combustion is lower (by about 200–300 deg depending on the fuel dose in the prechamber) than in the main chamber (Fig. 13a and 13b). Different conditions were recorded during methane combustion: much more favorable conditions prevailed in the prechamber, where temperatures about 100 deg higher were recorded.

A higher fuel dose in the prechamber increases the flame temperature during hydrogen combustion (Fig. 14a), while it decreases the temperature during methane combustion (Fig. 14b). This could mean that a significant amount of hydrogen leaves the prechamber even before ignition, and this dose should be increased. The same conclusion is reached by analyzing the pressure in the prechamber. The temperature distribution obtained corresponds to the adiabatic flame temperature, which is higher for hydrogen when using air as an oxidant.

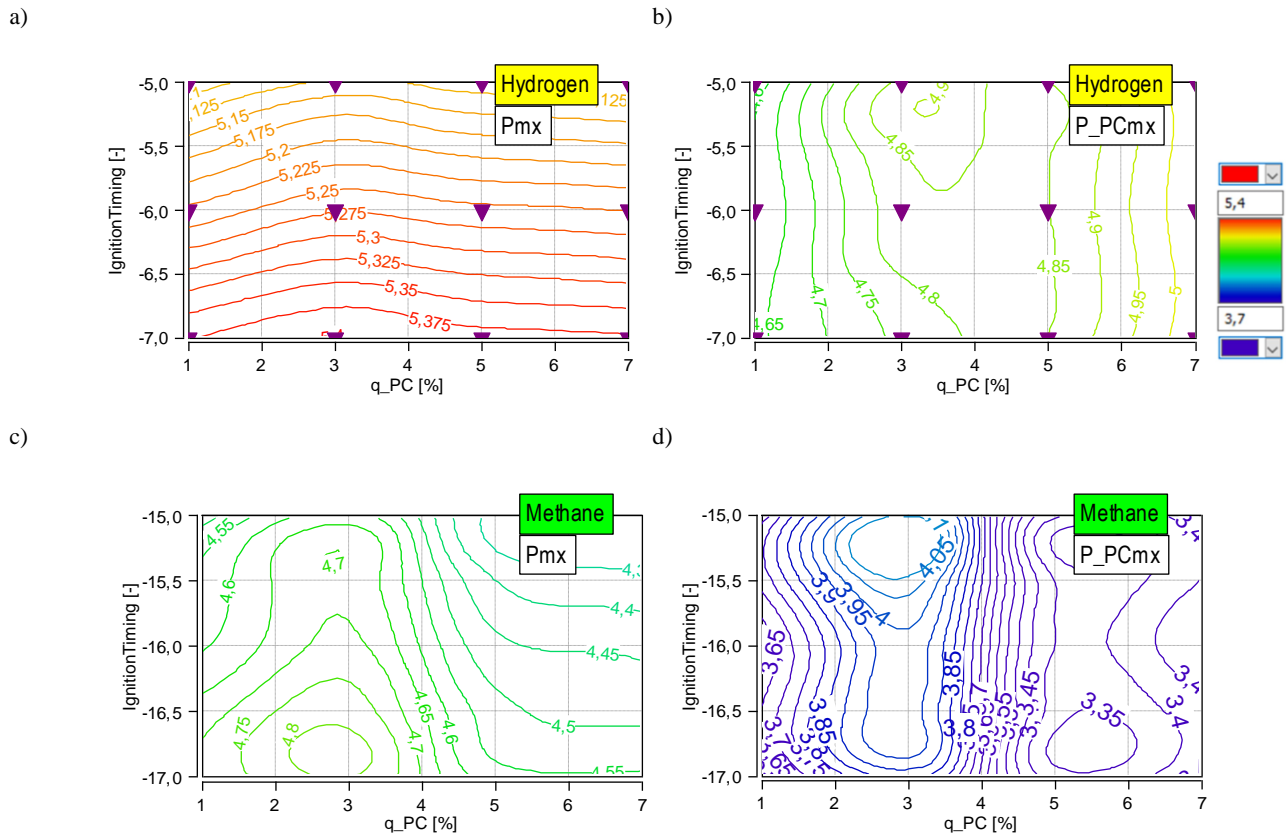


Fig.12. Cylinder pressure map: a) hydrogen combustion in the main chamber; b) hydrogen combustion in the pre-chamber, c) methane combustion in the main chamber, d) methane combustion in the pre-chamber

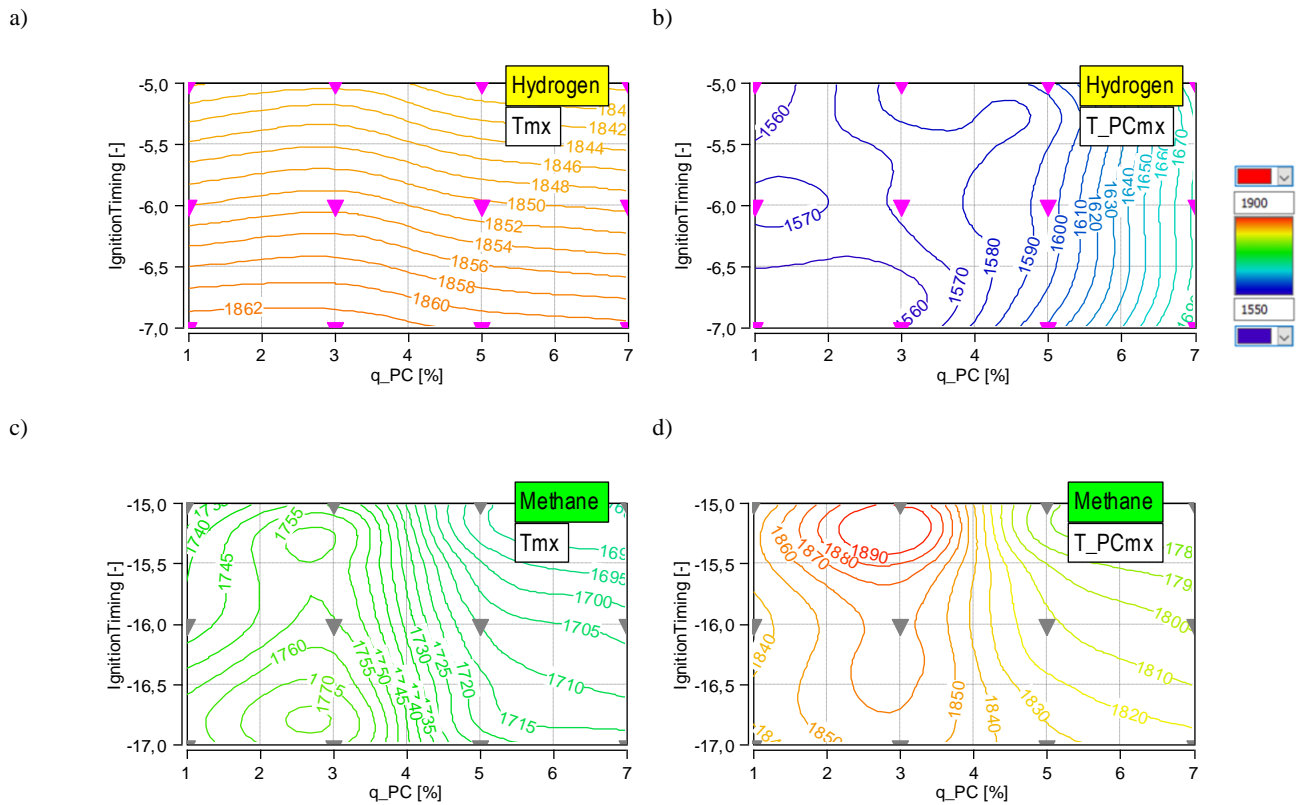


Fig. 13. Cylinder temperature maps: a) hydrogen combustion in the main chamber; b) hydrogen combustion in the pre-chamber, c) methane combustion in the main chamber, d) methane combustion in the pre-chamber

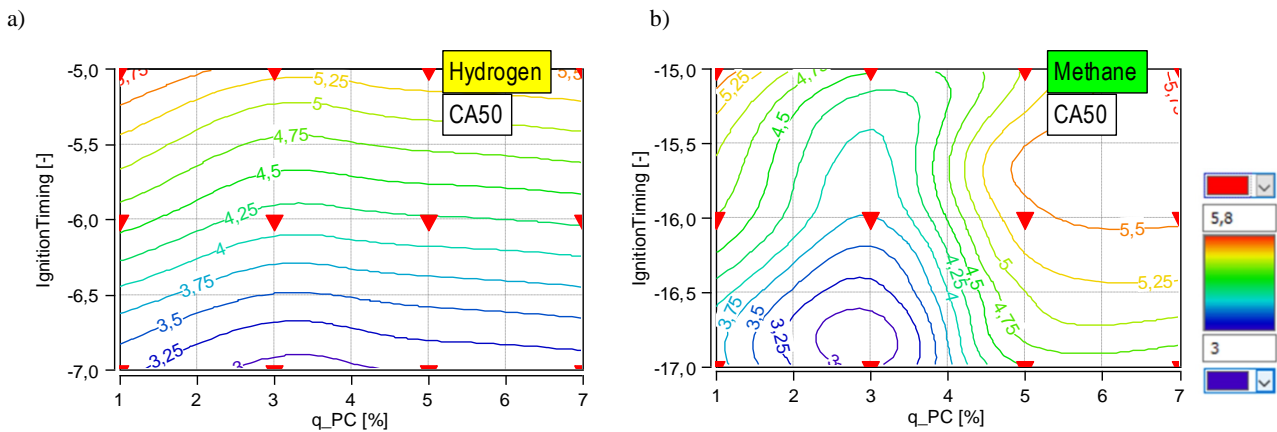


Fig. 14. Map of the combustion center: a) during hydrogen combustion, b) during methane combustion

The effect of the ignition timing and fuel dose injected into the PC on the center of combustion location, marked as CA50, is shown in Fig. 14. The nature of the changes are significantly different. Hydrogen supply with wide flammability limits results in no significant effect of fuel dose on CA50 (Fig. 14a). When methane is used, a change in the fuel proportion to PC above and below 3% causes a delay in the CA50 position (Fig. 14b).

Analyzing the effect of the ignition timing regardless of the fuel used, a classic trend was obtained; as the ignition timing advances, the CoC is closer to TDC. For the analyzed operating field, the characteristic point is the proportion of 3% dose to PC. In the case of both fuels for the aforementioned dose share, CA50 occurs earliest.

## 6. Summary

The information contained in the article focuses on the hydrogen and methane combustion analysis of the Turbulent Jet Ignition system with an active pre-combustion chamber. The variation of the process conditions was pointed out, and varied results were obtained with respect to cylinder pressure, temperature and other indicators.

The ignition timing in the prechamber during hydrogen and methane combustion causes equal percentage changes in cylinder pressure: a 2°CA change in ignition causes a change in Pmx of about 5%.

Changing the fuel dose delivery into the prechamber has a much stronger effect on the combustion pressure of methane than that of hydrogen.

The intensity of hydrogen combustion is much higher than methane combustion. A higher maximum pressure in the prechamber is obtained and a much higher intensity of heat release is observed. Maintaining the center of combustion in the same position for both fuels requires delaying the ignition advance an-

gle of hydrogen by about 10 deg compared to the methane combustion.

Center of combustion analysis indicates that there are different relationships during combustion of the two fuels. Changing the ignition angle during hydrogen combustion changes the combustion center, but the contribution of the fuel dose rate in the prechamber does not affect this indicator. During methane combustion, both the ignition angle and the fuel dose rate are important. At high ignition advance angles, increasing the dose increases the angle of the combustion center. With significant ignition advance, increasing the fuel dose to PC shifts the center of combustion away.

The presented simulation studies do not fully cover the issue related to the combustion of methane and hydrogen in two-stage combustion systems. Further research work on hydrogen combustion may include the following topics:

- center of combustion optimization analysis for various excess air ratios
- influence of the pre-chamber hole number and location on the combustion process quality
- pre-chamber volume optimization in terms of overall engine efficiency
- possibilities of multi-fuel combustion (hydrogen, methane, propane, butane) considering different pre-chamber fuel injection strategies
- combustion of ammonia in a two-stage system including hydrogen supply to the prechamber
- evaluation of knock combustion in relation to the restricted excess air ratio and the possibility of using an exhaust gas recirculation system
- optimization of the excess air ratio by applying supercharging to the quality of the combustion process.

## Acknowledgements

This work has been done under AVL University Partnership Program.

## Nomenclature

CI	compression ignition	OPEC	Organization of the Petroleum Exporting Countries
DI	direct injection	P	pressure
EOC	end of combustion	PC	prechamber
HD	heavy-duty engine	PCSI	Pre-Chamber Spark Ignited
HR	heat release	PFI	port fuel injection
HRR	heat release rate (or rate of heat release – ROHR)	RCTJI	reactivity-controlled turbulent jet ignition
IMEP	indicating mean effective pressure	SOC	start of combustion
LPG	liquefied petroleum gas	TJI	Turbulent Jet Ignition
MC	main chamber	q	fuel dose
MFB	mass fraction burned	$\lambda$	air excess ratio
MFB50	center of combustion (or CoC, CA50)	mx	index max

## Bibliography

- [1] Accurize Market Research Reports & Consulting Services <https://www accurizemarketresearch.com> (accessed on 1.09.2023)
- [2] Alvarez ECE, Couto GE, Roso VR, Thiriet AB, Valle RM. A review of prechamber ignition systems as lean combustion technology for SI engines. *Appl Therm Eng.* 2018;128:107-120. <https://doi.org/10.1016/j.applthermaleng.2017.08.118>
- [3] Cernat A, Pana C, Negurescu N, Nutu C, Fuiurescu D, Lazaroiu G. Aspects of an experimental study of hydrogen use at automotive diesel engine. *Heliyon.* 2023; 9:w13889. <https://doi.org/10.1016/j.heliyon.2023.e13889>
- [4] Cummins Inc. Debuts 15-Liter Hydrogen Engine at ACT EXPO. 2022.05.09. <https://www.cummins.com> (accessed on 1.06.2023)
- [5] Hajjari M, Tabatabaei M, Aghbashlo M, Ghanavati H. A review on the prospects of sustainable biodiesel production: a global scenario with an emphasis on wasteoil biodiesel utilization. *Renew Sustain Energy Rev.* 2017; 72:445-464. <https://doi.org/10.1016/j.rser.2017.01.034>
- [6] Han M. The effects of synthetically designed diesel fuel properties – cetane number, aromatic content, distillation temperature, on low-temperature diesel combustion. *Fuel.* 2013; 109:512-519. <https://doi.org/10.1016/j.fuel.2013.03.039>
- [7] Health and Safety Laboratory, injecting hydrogen into the gas network – a literature search. *Research Report.* 2015;1047.
- [8] Hosseini SH, Tsolakis A, Alagumalai A, Mahian O, Lam SS, Pan J et al. Use of hydrogen in dual-fuel diesel engines. *Prog Energy Combust.* 2023;98:101100. <https://doi.org/10.1016/j.pecs.2023.101100>
- [9] Hountalas DT, Kouremenos AD. Development and application of a fully automatic troubleshooting method for large marine diesel engines. *Appl Therm Eng.* 1999; 19:299-324. [https://doi.org/10.1016/S1359-4311\(98\)00048-9](https://doi.org/10.1016/S1359-4311(98)00048-9)
- [10] Hydrogen and Fuel Cell Technologies Office. Office of Energy Efficiency & Renewable Energy. February H2IQ Hour: Overview of hydrogen internal combustion engine (H2ICE) Technologies. <https://www.energy.gov/eere/fuelcells> (accessed on 1.06.2023)
- [11] Incer-Valverde J, Korayem A, Tsatsaronis G, Morosuk T. “Colors” of hydrogen: Definitions and carbon intensity. *Energ Convers Manage.* 2023;291:117294. <https://doi.org/10.1016/j.enconman.2023.117294>
- [12] Koten H. Hydrogen effects on the diesel engine performance and emissions. *Int J Hydrogen Energ.* 2018; 43(22):10511-10519. <https://doi.org/10.1016/j.ijhydene.2018.04.146>
- [13] Liu J, Dumitrescu CE. Single and double Wiebe function combustion model for a heavy-duty diesel engine retrofitted to natural-gas spark-ignition. *Appl Energy.* 2019;248:95-103. <https://doi.org/10.1016/j.apenergy.2019.04.098>
- [14] Liu Z, Wei H, Shu G, Zhou L. Ammonia-hydrogen engine with reactivity-controlled turbulent jet ignition (RCTJI). *Fuel.* 2023;348:128580. <https://doi.org/10.1016/j.fuel.2023.128580>
- [15] Makaryan IA, Sedov IV, Salgansky EA, Arutyunov AV, Arutyunov VS. A comprehensive review on the prospects of using hydrogen–methane blends: challenges and opportunities. *Energies.* 2022;15:2265. <https://doi.org/10.3390/en15062265>
- [16] Meske P, Schmidt K, Shiba H, Capellmann D, Retzlaff M, Zimmer P et al. Component and combustion optimization of a hydrogen internal combustion engine to reach high specific power for heavy-duty applications. *SAE Technical Paper 2023-32-0038.* 2023. <https://doi.org/10.4271/2023-32-0038>
- [17] Peters N, Bunce M. Active pre-chamber as a technology for addressing fuel slip and its associated challenges to lambda estimation in hydrogen ICEs. *SAE Technical Paper 2023-32-0041.* 2023. <https://doi.org/10.4271/2023-32-0041>
- [18] Qi Y, Liu W, Liu S, Wang W, Peng Y, Wang Z. A review on ammonia-hydrogen fueled internal combustion engines. *eTransportation.* 2023;18:100288. <https://doi.org/10.1016/j.etrans.2023.100288>
- [19] Ramsay CJ, Dinesh KKJR. Numerical modelling of a heavy-duty diesel-hydrogen dual-fuel engine with late high pressure hydrogen direct injection and diesel pilot. *Int J Hydrogen Energ.* <https://doi.org/10.1016/j.ijhydene.2023.09.019>

- [20] Ravaglioli V, Moro D, Serra G, Ponti F. MFB50 on-board evaluation based on a zero-dimensional ROHR model. SAE Technical Paper 2011-01-1420. 2011. <https://doi.org/10.4271/2011-01-1420>
- [21] Schäfer P. Keyou Establishing an H2 Development and Test Center. <https://www.springerprofessional.de> (accessed on 1.06.2023)
- [22] Schiro F, Stoppato A, Benato A. Modelling and analyzing the impact of hydrogen enriched natural gas on domestic gas boilers in a decarbonization perspective. Carbon Resources Conversion. 2020;122-129. <https://doi.org/10.1016/j.crcon.2020.08.001>
- [23] Statista – The portal for statistics. 2019. <https://www.statista.com>
- [24] Tapping the potential within 100% hydrogen-powered engines. <https://www.yamaha-motor.eu> (accessed on 1.06.2023)
- [25] Tomaschitz M. AVL RACETECH builds hydrogen combustion engine for motorsport. <https://www.avl.com> (accessed on 1.06.2023)
- [26] Tsukamoto Y, Tanno S, Miyamoto Y, Sakai H, Omura T, Takahashi D. Analysis of the effect of hydrogen combustion characteristics on engine performance. SAE Technical Paper 2023-32-0039. 2023. <https://doi.org/10.4271/2023-32-0039>
- [27] Tutak W, Grab-Rogaliński K, Jamrozik A. Combustion and emission characteristics of a biodiesel-hydrogen dual-fuel engine. Appl Sci. 2020;10:1082. <https://doi.org/10.3390/app10031082>
- [28] Wimmer A, Wallner T, Ringler J, Gerbig F. H2-direct injection – a highly promising combustion concept. SAE Technical Paper 2005-01-0108. 2005. <https://doi.org/10.4271/2005-01-0108>
- [29] Winangun K, Setiyawan A, Sudarmanta B, Puspitasari I, Dewi EL. Investigation on the properties of a bio-diesel-hydrogen mixture on the combustion characteristics of a diesel engine. Case Studies in Chemical and Environmental Engineering. 2023;8:100445. <https://doi.org/10.1016/j.cscee.2023.100445>
- [30] Winangun K, Setiyawan A, Sudarmanta B. The combustion characteristics and performance of a Diesel Dual-Fuel (DDF) engine fueled by palm oil biodiesel and hydrogen gas. Case Stud Therm Eng. 2023;42:102755. <https://doi.org/10.1016/j.csite.2023.102755>
- [31] Wu Y-Y, Wang JH, Mir FM. Improving the thermal efficiency of the homogeneous charge compression ignition engine by using various combustion patterns. Energies. 2018;11(11): 3002. <https://doi.org/10.3390/en11113002>
- [32] Yadav K, Anirbid S. Hydrogen compressed natural gas and liquefied compressed natural gas: fuels for future. PDP J Energy Manag. 2017;2:29-33. <https://www.pdpu.ac.in/downloads/3%20Hydrogen-Compressed-Natural-Gas.pdf> (accessed on 14 January 2022).
- [33] Yilmaz I. Effects of hydrogen addition to the intake air on performance and emissions of common rail diesel engine. Energy. 2018;142:1104-1113. <https://doi.org/10.1016/j.energy.2017.10.018>
- [34] Yip HL, Srna A, Yuen ACY, Kook S, Taylor RA, Yeoh GH et al. A review of hydrogen direct injection for internal combustion engines: Towards carbon-free combustion. Appl Sci. 2019;9:1-30. <https://doi.org/10.3390/app9224842>
- [35] Yuvenda D, Sudarmanta B, Wahjudi A, Muraza O. Improved combustion performances and lowered emissions of CNG-diesel dual fuel engine under low load by optimizing CNG injection parameters. Fuel. 2020; 269: 117202. <https://doi.org/10.1016/j.fuel.2020.117202>